Elastic effects in intercalation compounds: Comparison of lithium in graphite and TiS_2

J. E. Fischer* and H. J. Kim†
Laboratory for Research on the Structure of Matter, University of Pennsylvania, Philadelphia, Pennsylvania 19104
(Received 15 August 1986)

We compare the concentration dependence of stage-1 package thicknesses for the intercalation compound families Li_xC_6 and Li_xTiS_2 in order to study the influence of host elastic properties on staging. In both families the data suggest that local host-layer distortions around isolated intercalates are important, an elastic model based on rigid layers giving a poor fit. The decay lengths for local distortions are 5 and 7 Å, respectively, for graphite and TiS_2. We argue that a more concentrated strain field associated with the smaller decay length gives rise to a larger value of U_0, the effective in-plane two-body attractive potential, for Li in graphite relative to TiS_2. This in turn explains qualitatively why Li_xC_6 exhibits high stages at 300 K for various x while Li_xTiS_2 is restricted to stage 1.

Intercalation compounds consist of alternating sequences of two-dimensional (2D) host and guest layers. The most dramatic structural feature of these materials is staging, defined as the formation of long-period one-dimensional (1D) superlattices along the c axis in which n host layers and 1 guest layer alternate in a regular array. Safran described the phenomenon as resulting from competition between long-ranged out-of-plane repulsive and short-ranged in-plane attractive interactions.[1] In the simple Ising-like phase diagram, the lattice-gas configurational entropy drives the system from "ferromagnetically ordered" high-stage structures at low T to the "paramagnetic" dilute stage-1 structure at high T. The model is universal in the sense that transition temperatures scale with U_0 independent of host properties, where U_0 is the effective two-body attractive interaction between occupied sites in the same gallery. It is thus something of a mystery why staging is ubiquitous in graphite intercalation compounds while the same species in other layer hosts are generally limited to stage-1 sequences. This paper is a first attempt to explain the mystery, by considering the effect of different host properties on U_0 for the same intercalate. There are two fundamental microscopic interactions which control the energetics of intercalation compounds—elastic and electrostatic. We focus here on the former since a discussion of the latter involves details of host-crystal energy band structures.

Elastic interactions play an important role in the structural chemistry of intercalation compounds. These can be modeled either as a collection of rigid planes held together by Hooke's-law springs[2] or by local dipole strain fields arising from the deformation of host layers flanking an intercalate, or "island" of intercalates.[3] The latter viewpoint has the advantage that it accounts in principle for contributions to both the interlayer and intralayer energetics—the relaxation of these distortions away from the locally expanded host at an occupied site determines the dependence of the average filled gallery thickness I_c on the fractional occupancy of lattice-gas sites within a single gallery, while the magnitude and range of the strain field defines the elastic contribution to U_0. The latter in turn sets the scale for staging transitions as a function of T, chemical potential μ, relative concentration x, or hydrostatic pressure. To the extent that elastic effects dominate, one would thus expect compounds exhibiting similar I_c versus x behavior to have similar U_0 since both are controlled by the same microscopic phenomenon. Conversely, if a given intercalate exhibits different high stages as a function of μ or x at fixed (T,P) in host A, but only stage 1 in host B, the different elastic properties of A and B would be implicated. A complete description of these distortions requires knowledge of C_{33} and the layer-bending modulus to account for both the rigid-layer c-axis expansion at large x when the distortions overlap, and the isolated single-layer distortions at small x.

Lithium may be intercalated into graphite and many transition-metal dichalcogenides. Comparison of the different T-dependent staging behavior of Li in various hosts, in the framework of the original Safran model,[4] suggests that for graphite, $NbSe_2$, and TiS_2 U_0 is respectively >1500 K, of order 1000 K, and <750 K.[5] The extent to which these differences may be understood in terms of different host elastic properties is addressed here by comparing the dependence of I_c on x for two sets of stage-1 compounds Li_xC_6 and Li_xTiS_2. The stage-1 restriction ensures unambiguous values for the average thickness of an occupied gallery, obtained directly from diffraction peaks rather than relying on high-stage data and the assumption that the thickness of empty galleries is unaffected by intercalation.[6] For TiS_2 this restriction is satisfied by *in situ* x-ray $(00L)$ diffraction during solution intercalation at 300 K (Ref. 2) since the Safran phase boundary lies below 300 K for all x. In graphite, on the other hand, we are obliged to perform $(00L)$ scans on samples of different x at some high T above which all samples have transformed to the dilute stage-1 phase.[7]

The choice of Li is dictated by two considerations: the transitions in graphite occur at accessible temperatures over most of the range of x, and Li satisfies the lattice-gas assumption for TiS_2 (Ref. 8) and (probably) graphite.[9]

Samples of Li_xC_6 were prepared by immersing 0.5-g pieces of highly oriented pyrolytic graphite (HOPG) in molten Li-Na alloys, the value of x at equilibrium being controlled by Li concentration and temperature.[10] After intercalation, excess metal was removed by carving and polishing, and the samples were encapsulated by welding into 0.001-in.-thick stainless-steel foil envelopes. All operations were performed in an argon atmosphere. Neutron diffraction profiles were measured as a function of T using the $H4$-S triple-axis spectrometer at Brookhaven; the relative accuracy in I_c is estimated as ± 0.003Å. The low Li vapor pressure and small free volume ensured that deintercalation did not occur during the measurements, confirmed by noting that the 300-K $(00L)$ diffractograms were reproducible before and after high-T runs as long as T does not exceed 730 K. The "failure mode" above 730 K is the slow conversion of the intercalation compound to lithium carbide Li_2C_2, as opposed to loss of Li from the sample.[11] Figure 1 shows the transformation from a mixed stage-$(1+2)$ to pure stage-1 phase with increasing T, in samples of Li_xC_6 with $0.69 < x < 0.95$. We determined x crystallographically from the structure factors of LiC_6 and LiC_{12} and the low-T relative integrated intensities of the respective $(00L)$ peaks. These values agree sometimes but not always with chemical analysis, attributable to the incorporation of Li-Na alloy in cracks in some of the samples. These data confirm that the Safran boundary has $dT_c/dx < 0$ for this range of x. We note also that the transition is markedly broadened as the low-T stage-2 fraction decreases. Hysteresis (not shown) suggests first-order transitions, the smearing depending inversely on Li vacancy concentration. Above these staging transitions the Li sublattice is still three-dimensionally ordered showing the same $\sqrt{3}\times\sqrt{3}$ in-plane superlattices as LiC_6 with interlayer correlation lengths of 100 Å or more. Figure 2 shows the corresponding family of three-dimensional (3D) melting transitions at higher temperatures, including results for $x=1$.[12] In contrast to the ferromagnetic-paramagnetic phase boundary, $dT_c/dx > 0$ for the melting transitions—the higher the vacancy concentration the lower the melting point—and the ordered phase can support a vacancy concentration of at least 30%. Here again the data suggest smeared first-order transitions, but the systematic dependence of smearing on x for the melting transitions is reversed with respect to that of the staging transitions. These aspects of the results will be presented in detail elsewhere.

We chose 700 K as the reference temperature for I_c versus x, having verified that the stage-1 repeat distance is not affected by the melting transition. Figure 3 shows the results, including data from dilute samples.[7] Measurements on duplicate samples near $x=0.1$ and 0.7 gave excellent reproducibility. In the range $0.2 < x < 0.4$ we are unable to reach pure stage-1 phase with increasing T due to the extreme stability of the high-entropy dilute stage-2 phase "LIC_{16}."[13,14] Despite this limitation we clearly see a monotonic increase at small x, saturating near $x=0.7$ and then leveling off. As shown in the insets, this behavior suggests that at low x the diffraction averages over the C-layer distortions to give a d spacing which increases as the distortions become more dense and finally overlap. At $x=0.7$ the overlap is sufficient to "heal" the distortions, thus the C layers are flat and I_c achieves its maximum value even though there are still 30% vacant sites. At $x=0.7$ the average Li-Li in-plane separation is 5 Å which we infer as the approximate decay length of C-layer distortions around an isolated Li intercalate.

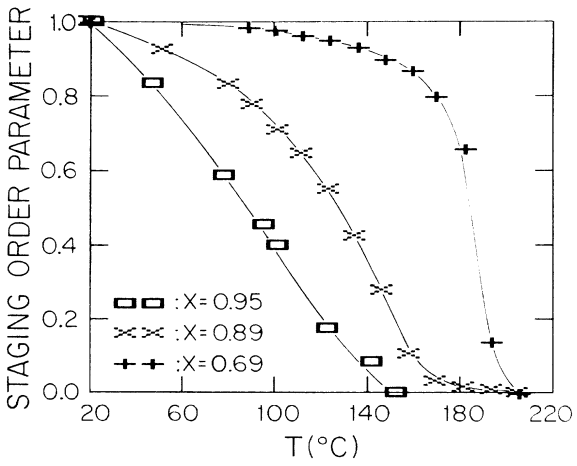

FIG. 1. Staging transitions in Li_xC_6 from mixed stage $(1+2)$ to pure dilute stage 1, determined from $(00L)$ neutron diffraction integrated intensities and plotted as percent stage 2 remaining at T normalized to 20 C. Solid curves are guides to the eye.

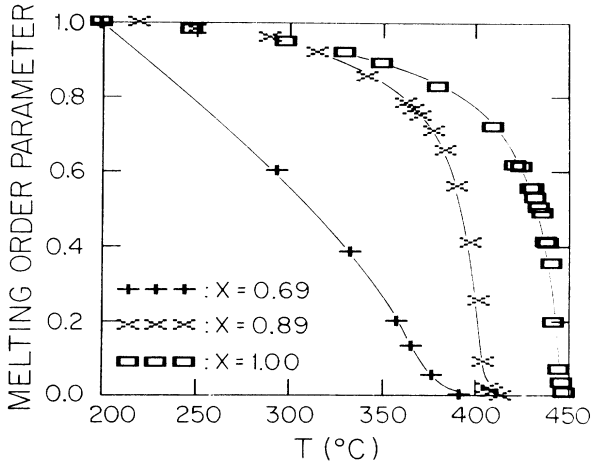

FIG. 2. Melting transitions in Li_xC_6 from 3D-ordered $\sqrt{3}\times\sqrt{3}$ in-plane superlattice with stage-1 $A\alpha A\alpha A\alpha$ stacking, to (presumed) lattice gas, determined from powder-averaged (HKO) neutron diffraction integrated intensities and plotted as percent first-order superlattice peak remaining at T normalized to 200 C. Data for $x=1$ from Ref. 12. Solid curves are guides to the eye.

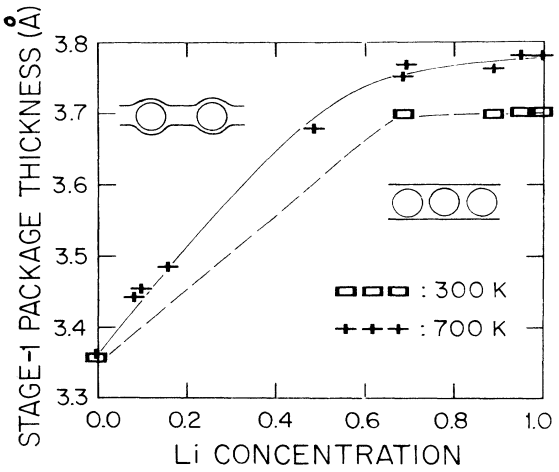

FIG. 3. Stage-1 package thickness vs x in Li_xC_6, measured directly from the (001) peak position at 700 K on pure stage-1 samples of varying Li density, (+). Data also shown for the LiC fraction in samples with $x > 0.5$ (mixed stage 1 and stage 2) at 300 K, (□). Solid lines are guides to the eye. Insets describe local host-layer distortions which are isolated at low x (top left) but overlap as $x \rightarrow 1$ to give flat host layers (lower right).

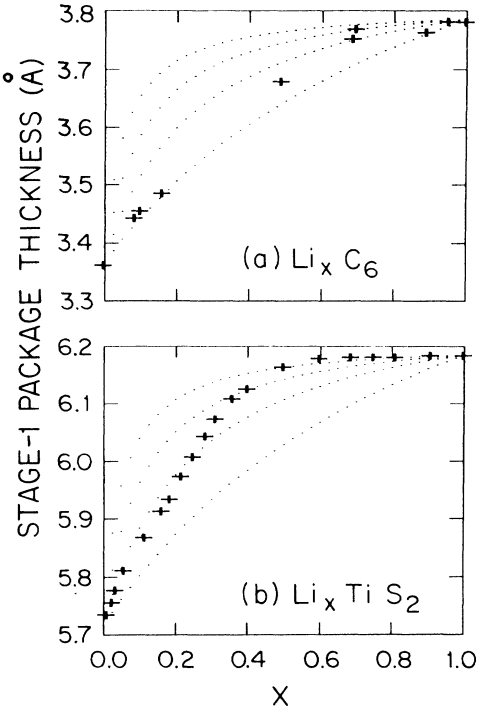

FIG. 4. Comparison of experiment and theory for (a) Li_xC_6 and (b) Li_xTiS_2 (data from Ref. 2). Model results (Ref. 2) given for spring constant ratios 0.05, 0.1, 0.2, and 0.5 reading from top down (see the text). The maximum c-axis expansion is 0.45 Å in both hosts, saturating at lower x (greater in-plane Li-Li separation) in TiS_2 compared to graphite. Neither data are represented correctly by the rigid-layer model.

Also included in Fig. 3 are data points obtained from the stage-1 reflections in mixed-phase samples at 300 K, well below the staging transitions shown in Fig. 1. Within experimental error there is (sensibly) no variation of I_c with x, confirming that the low-T stage-1 component in samples with $0.69 < x < 1.0$ is indeed LiC_6 with all sites occupied at low T. Comparison with the 300 and 700 K values at $x = 0$ shows that the c-axis thermal expansion coefficient of LiC_6 substantially exceeds that of graphite, continuing the trend of increasing c-axis expansion coefficient with decreasing intercalate mass found by Hardcastle and Zabel.[15]

The data of Fig. 3 lends qualitative support to the local distortion picture. The rigid-layer model of Dahn *et al.*[2] (the first to account quantitatively for elastic effects) takes the opposite point of view. Empty galleries are held together by springs of spring constant K while host layers flanking an intercalate are represented by stronger but longer springs k, the ratio $K/k < 1$; all layers are assumed to be flat at all x. In Fig. 4 we compare the Li_xC_6 and Li_xTiS_2 data with the rigid-layer model, modified as suggested by Safran[1] to keep the total number of springs constant. In neither case does the model give a reasonable fit with a single value of K/k, implying that the spring constants themselves are concentration dependent. This is precisely the implication of the local distortion viewpoint. The more complete data for Li_xTiS_2 [Fig. 4(b)] show very clearly the saturation of I_c versus x, occurring at a lower value than in graphite [Fig. 4(a)]. In the rigid-layer model this says that the galleries in TiS_2 are propped fully apart with fewer Li per unit area than in graphite. The more useful conclusion for our purposes is that the distortions around individual atoms fall off more slowly with distance in TiS_2 as compared to graphite and thus overlap at a larger Li-Li separation. From either viewpoint the TiS_2 "layers" are obviously stiffer than graphite, which should be reflected also in differences in layer bending moduli. (One could also envision a critical stiffening of the bending modulus of the compound at x corresponding to saturation of I_c.) The stiffness of TiS_2 "layers" is no doubt enhanced by the nonplanar covalent bonds among the constituent metal and chalcogen atoms.

We estimate the in-plane extent of host-layer distortions as being equal to the average Li-Li separation at the concentration where I_c versus x saturates. For graphite $a_0 = 2.46$ Å and the Li-Li distance at $x = 1$ is $\sqrt{3}a_0 = 4.26$ Å; at $x = 0.7$ this increases to 5 Å which is close to the distance between the sites on a 2×2 superlattice. For TiS_2 $a_0 = 3.41$ Å and is equal to the Li-Li separation at $x = 1$, increasing at $x = 0.5$ to 7 Å, again close to the 2×2 separation for this lattice. We interpret this to mean that lattice-gas disorder in dilute phases constrains the in-plane distortions to be coherent with the host structure, rather than taking on any value as for a uniform elastic sheet. Thus the commensurability between guest and host reveals itself even indirectly through the host-layer distortions.

The relatively slow damping of local distortions in TiS_2 also implies a smaller value of U_0 (albeit a longer range) compared to graphite. The out-of-plane expansion is the

same in both hosts, but the associated strain field is more diffuse in TiS_2 (for perfectly stiff layers there would be no distortions hence no in-plane attractive elastic interaction). This is entirely consistent with differences in T-dependent staging exhibited by Li in these two hosts. We assume that the strain energy goes roughly as the inverse square of the planar dimension of a distortion, whence the ratio $\frac{5}{7}$ gives $U_0(\text{graphite}) = 2U_0(TiS)_2$ in good agreement with estimates based on staging behavior versus T.[5] Furthermore, the trends with alkali size in a given host are in the right direction for the distorted-layer picture. From Fig. 1 we estimate the midpoint of a $(1+2)\rightarrow(1)$ staging transition in $Li_{0.8}C_6$ to be 440 K, while the corresponding transition in $Cs_{0.8}C_8$ occurs at 600 K.[16] Assuming similar overall shapes for the phase boundaries, U_0(Cs-graphite) exceeds U_0(Li-graphite) by $\sim 50\%$ consistent with the differences in local expansions of 70% and 10%, respectively. Similarly for TiS_2, high stages are found at 300 K for Cs but not for Li.[17]

At this point one may well ask: What about electrostatic effects? We have previously presented two examples in which the c-axis spacing *decreases* slightly as x increases from 0.7 to 1.0, attributed to the increase in areal charge density enhancing the first neighbor attraction between oppositely charged sheets. Stage-1 graphite bisulfate contracts along c by 0.1 Å as the charge density increases from 75% to 100% of the ionic limit,[18] while stage-2 Li-graphite contracts by ~ 0.03 Å in response to a similar increase in gallery filling.[13] The former experiment is complicated by the steric effect of the "neutral spacers," while the small expansion in stage-2 Li-graphite is ambiguous due to the presence of empty galleries of unknown thickness (it is entirely possible that the interlayer C-Li distance is the same in both phases[19]). Theoretical work to date has either ignored the structural details to make tractable the problem of incorporating finite temperature[4,14,20] or has focussed on determining the ground-state structure for specific compositions.[9,21] Electrostatic forces certainly dominate the interlayer interactions in pure high stages since the interlayer strains vanish for a perfect sequence.[3] They are also important in-plane at short range (large x) (Ref. 9) since the interlayer strains also vanish when the local distortions overlap. Conversely, we have shown that the effect of local distortions is most dramatic at low x. A complete staging phase diagram may require both effects to properly account for high and low "coverages" at all temperatures.

We acknowledge useful discussions with Paul Heiney and Samuel Safran. This work was supported by the National Science Foundation Materials Research Laboratory Program under Grant No. DMR-8519059 and by the Department of Energy under Grant DEFG02-86ER45254. The High Flux Beam Reactor is operated at Brookhaven under support from the Department of Energy (DOE) Division of Materials Science under Contract No. DEAC02-76CH00016.

---

*Also at Materials Science and Engineering Department, University of Pennsylvania, Philadelphia, PA 19104.

†Also at Physics Department, University of Pennsylvania, Philadelphia PA 19104. Current address: Institut Laue-Langevin, 156X, F-38042 Grenoble, France.

[1]For an up-to-date review see S. A. Safran, in *Solid State Physics,* edited by F. Seitz, D. Turnbull, and H. Ehrenreich (Academic, New York, in press).

[2]J. R. Dahn, D. C. Dahn, and R. R. Haering, Solid State Commun. **42**, 179 (1982).

[3]S. A. Safran and D. R. Hamann, Phys. Rev. Lett. **42**, 1410 (1979).

[4]S. A. Safran, Phys. Rev. Lett. **44**, 937 (1980).

[5]J. E. Fischer, C. D. Fuerst, and K. C. Woo, Synth. Met. **7**, 1 (1982).

[6]A. Herold, in *Intercalated Layer Materials,* edited by F. Levy (Reidel, Boston, 1979), p. 321.

[7]K. C. Woo, H. Mertwoy, J. E. Fischer, W. A. Kamitakahara, and D. S. Robinson, Phys. Rev. B **27**, 7831 (1983).

[8]B. Silbernagel, Mater. Sci. Eng. **31**, 281 (1977).

[9]D. P. DiVincenzo and E. J. Mele, Phys. Rev. B **27**, 2458 (1983).

[10]S. Basu, C. Zeller, P. Flanders, C. D. Fuerst, W. D. Johnson, and J. E. Fischer, Mater. Sci. Eng. **38**, 275 (1979).

[11]D. Guerard and A. Herold, Carbon **13**, 337 (1975).

[12]J. Rossat-Mignod, A. Wiedenmann, K. C. Woo, J. W. Milliken, and J. E. Fischer, Solid State Commun. **44**, 1339 (1982).

[13]K. C. Woo, W. A. Kamitakahara, D. P. DiVincenzo, D. S. Robinson, H. Mertwoy, J. W. Milliken, and J.E. Fischer, Phys. Rev. Lett. **50**, 182 (1983).

[14]D. P. DiVincenzo and T. C. Koch, Phys. Rev. B **30**, 7092 (1984).

[15]S. E. Hardcastle and H. Zabel, Phys. Rev. B **27**, 6363 (1983).

[16]R. Clarke, N. Caswell, and S. A. Solin, Phys. Rev. Lett. **42**, 61 (1979).

[17]J. Rouxel, in *Intercalated Layer Materials,* Ref. 6, p. 201.

[18]A. Metrot and J. E. Fischer, Synth. Met. **3**, 201 (1981).

[19]N. Caswell, S. A. Solin, T. M. Hayes, and S. J. Hunter, Physica **99B**, 463 (1980).

[20]S. E. Millman and G. Kirczenow, Phys. Rev. B **28**, 3482 (1983).

[21]H. Miyazaki, Y. Kuramoto, and C. Horie, J. Phys. Soc. Jpn. **53**, 1380 (1984).